Nematic topological line defects as optical waveguides

Miha Čančula[a], Miha Ravnik[a] and Slobodan Žumer*[ab]
[a]Faculty of Mathematics and Physics, University of Ljubljana, Jadranska 19,
SI-1000 Ljubljana, Slovenia;
[b]Jožef Stefan Institute, Jamova 39,
SI-1000, Ljubljana, Slovenia

ABSTRACT

Liquid crystals are starting to attract attention for applications beyond the display technology. Their high birefringence, softness, and possibility to form complex topological defect structures allow for easy light manipulation in systems ranging from cholesteric lasers to droplet resonators and wave guides. Recent interest in light-induced topological defects and light propagation along the defects stimulated us to develop a customized version of the Finite-Difference Time-Domain (FDTD) method for solving Maxwell's equations on a discrete time & space lattice. Here, we present an overview of our recent simulations, modeling the time-evolution of electromagnetic fields along birefringent structures in nematic liquid crystals, specifically light propagation along nematic defect lines. In the regime of high light intensity beams the modelling approach includes also a light induced modification of local nematic ordering obtained via a q-tensor free energy minimization procedure. We show how topological invariants of the nematic and polarization fields combine and also affect the beam intensity profile. Finally, off-axis propagation of beams with respect to the defect lines is considered.

Keywords: topological defects, nematic disclinations, wave guiding, polarization profile, FDTD method, self-reshaping optical beam

INTRODUCTION

Light beams characterized by complex spatial modulation of both intensity and polarization profiles [1-3] are essential for numerous optical and photonic applications [4-8]. These vectorial beams are usually generated from simple linearly polarized laser beams by using conical Brewster prisms [9], few-mode fibers [10], or phase modulators [11].

Liquid crystals are central materials of modern displays due to their birefringence and high susceptibility to external control by electric fields. Recent search for-beyond-the-display applications of liquid crystal is partially focused on topological aspects of complex defect structures in confined nematic and chiral nematic phases [12-15]. These nematic defects can be singular points and lines or nonsingular solitonic structures [16,17]. Point defects are characterized by topological charge that is ascribed to a distinct spatial variation of the director field around the defect. Singular line defects, also called disclinations, and solitons like double twist cylinders are both characterized by a topological invariant - the winding number- which determines the local structure, e.g. in a plane. Specifically, it determines how many turns the director makes when encircling a defect line. As the director is a headless vector, the opposite directions are equivalent, and thus allows also for half-integer winding number of disclinations. In bulk nematic liquid crystals, only disclination lines with winding number $|s|=1/2$ are stable [16], as lines with higher winding numbers have higher free energy and decompose into multiple lines with lower strengths. Typically, in capillaries with homeotropic surfaces the director can escape in the third dimension (i.e. along the capillary axis), substituting splay deformation with bend, and removing the singular defect core to form an escaped radial structure [17].

Optical properties of liquid crystalline phases and defect structures at scales comparable to the wavelength of light enable strong coupling between the director and light polarization. It has been shown that nematic disclinations can induce singularities in the light field and generate vortex beams [18-20]. General manipulation of vectorial beams can be achieved using a liquid crystalline “q-plate” [21,22]. A light beam

Emerging Liquid Crystal Technologies X, edited by Liang-Chy Chien, Harry J. Coles,
Hirotsugu Kikuchi, Ivan I. Smalyukh · Proc. of SPIE Vol. 9384, 938402 · © 2015 SPIE
CCC code: 0277-786X/15/$18 · doi: 10.1117/12.2079096

carries spin that in the classical picture corresponds to the cylindrical polarization of light, and as well orbital angular momentum (OAM) if a phase vortex is present at the beam axis [23]. Transfer of angular momentum between spin and orbital degrees of freedom are usually achieved by q-plates [24,25]. On the other hand sufficiently strong light fields can locally reorient liquid crystal which allows for imprinting of defects in liquid crystals [14,26,27] or self-induced focusing that leads to formation of nematicons [28].

The paper is organized as follows. First we describe numerical modeling approach. Then modulation via nematic disclinations of initially Gaussian beams with linear and circular polarization into vector beams is presented. The modulation of laser beams by nematic defects is generalized for initial Laguerre-Gaussian beams with various intensity and polarization profiles. Beam profiles for mutually misaligned beam and nematic defect lines are shown. Finally, propagation of light along escaped nematic profile is considered.

NUMERICAL MODELING

We model the propagation of light using a custom-implemented Finite-Difference Time-Domain (FDTD) method [18,29]. This method calculates the time-derivatives of the electric (E) and magnetic field (H) directly using Maxwell's equations. The computation can be made more efficient by computing the values of E and H at different points in space and at different times. The symmetry of both equations is best exploited using the Yee lattice, where different field components are computed at different lattice sites [30,31]. However, the Yee lattice only gives an improvement when the permittivity tensor ε is diagonal, which is true in uniform solid crystals, but not in liquid crystals where the director can vary in space and time. Applying it to non-uniform fully-anisotropic ε can lead to instabilities [32]; therefore, we use our own, simpler lattice which is unconditionally stable even in complex permittivity tensor profiles. In our modeling, E and B are computed at distinct points in space and in time, but all three component of each field are computed at the same site. This incurs a performance penalty compared to the Yee lattice, but instead correctly supports fully anisotropic permittivity.

We introduce an external light beam on one side on the simulation cell. This is done by surrounding the cell with a buffer zone, and appropriately adding or removing the desired incident light field to each derivative in the Maxwell's equations that spans the cell border. Further, it is desired that the light which traverses the cell is released into free space with no reflection. To this end, we add a Perfectly Matched Layer (PML), a nonphysical material with high absorption and very low reflection at the interface for light at any frequency and at any angle [33]. The complete simulation cell, along with our lattice, is shown schematically in Fig. 1.

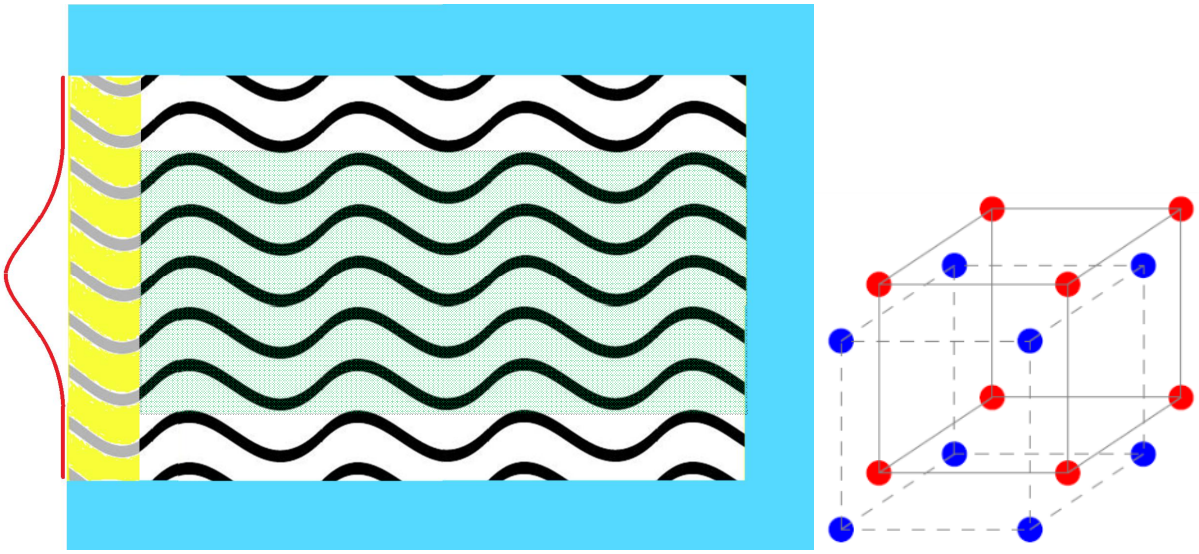

Figure 1. Schematic presentation of the numerical procedure. (left) Source area (intensity profile of the incoming beam), wave guiding area, absorption area that prevents reflection and allows smaller simulation box. (right) FDTD is implemented by a discretization of fields electric $\mathbf{E}(\mathbf{r}_n,t)$ and magnetic fields $\mathbf{B}(\mathbf{r}_m,t+t_o/2)$ on 2 spatially and time shifted cubic lattices

For light of low intensity, the liquid crystal director profile – i.e. the birefringence (dielectric permittivity) profile – can be assumed to be fixed and does not vary in time. However, for high-intensity light beams, the FDTD computation needs to be coupled with a model of the liquid crystal, such as Landau-de Gennes free energy minimization approach [34]. In reality, these processes occur on vastly different time scales; accurate FDTD modeling requires a time step no greater than one tenth of a wave period, measured in femtoseconds [29,35], while liquid crystal relaxation requires times on the order of milliseconds [16]. The following numerical parameters are used in calculations: wavelength 400nm, lattice resolution 30nm, simulation box size 400x400x768, birefringence +0.05, beam waist 6.0μm. The computation is performed using parallelized OpenCL code on Nvidia GTX Titan GPUs.

LINEAR INCIDENT POLARIZATION

We use the FDTD method described above to study the propagation of light beams along nematic disclination lines. For the case of low-intensity light beam, we assume the director profile stationary, so the relaxation of nematic profile (q-tensor) is omitted. The results show how the disclination line affects the topology of light. In particular, a linearly polarized Gaussian beam obtains a polarization defect at its axis, with the winding number of this defect equal to twice the winding number of the disclination line. An example with an s=-1/2 disclination line is shown in Figure 2.

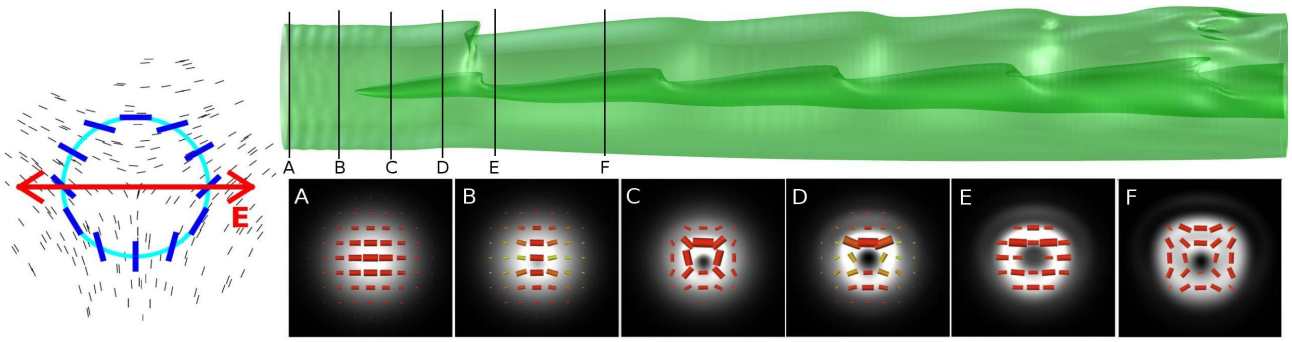

Figure 2. Intensity and polarization modulation of an (initially Gaussian) laser beam travelling along s=-1/2 disclination line. (left) The schematic shows the incident light polarization relative to the liquid crystal director profile. (right, top) A zero-intensity region forms at the defect core, as evidenced by the intensity isosurface. (right, bottom) Polarization profiles at different lengths travelled along the disclination line shows an effectively repeating transformation of the polarization profile. Two distinct defect states with winding numbers s=0 (at distances that are even multiples of $z=\lambda/2\Delta n$) and s=-1 (at odd multiples) are observed, and partially polarized intermediate states. Generally, initially linearly polarized incident light beam always attains a defect polarization profile (i.e. becomes a vector beam) with twice the winding number (charge) as the liquid crystal disclination line.

In Figure 2, the polarization profile of the beam changes as propagated along the disclination, effectively alternating between its original linear polarization and a defect profile with winding number -1. The occurrence of a pattern with a double winding number can be explained using the Jones calculus. Notably, the simple Jones matrix approach does not predict the zero-intensity region at the center which is necessary to prevent discontinuities in the electric and magnetic field. For proper study of the light propagation near and along liquid crystal defects, it is thus necessary to use more advanced approaches such as the FDTD method which properly accounts for wave phenomena including refraction.

The double winding number profile occurs in the polarization when the phase retardation δ between the ordinary and extraordinary components equals π, which happens at propagation length $z=\lambda/2\Delta n$. At this point, the light is locally linearly polarized as in the incident beam, but the direction of the polarization is effectively mirrored with respect to the optical axis, i.e. the director. The angle α between the director and the incident beam polarization varies in space, causing the resulting polarization to be space-dependent as well. The polarization angle is always twice that of the director due to the mirroring, causing the winding number to be twice that of the disclination line.

CIRCULAR INCIDENT POLARIZATION

If the incident light is polarized circularly rather than linearly, the spatial modulation of the polarization is via the nematic defect line is different. Here, at a certain distance along the disclination, light obtains a defect with the *same* winding number as the disclination. Interestingly, since the nematic disclination can have a half-integer winding number, this results in a half-integer light defect. Because the electric field is a vector, in principle it cannot form non-integer strength defects, which is an important topological difference between the electric field and light polarization fields. However, a half-integer defect can form in the polarization if it is combined with a half-integer phase vortex, which complies with the topological constrains caused by the vector nature of electric and magnetic fields. The resulting light polarization profiles are shown in Figure 3. Laguerre-Gaussian beams with either phase vortices [20, 21] or polarization defects [3, 22] are well-known solutions to the paraxial wave equation and have been studied extensively. However, we show that a disclination line can be used to produce hybrid Laguerre-Gaussian beams with both phase and polarization

singularities. The only topological constraint is that the sum of winding numbers of phase and polarization defects is an integer, while each number by itself can be a half-integer.

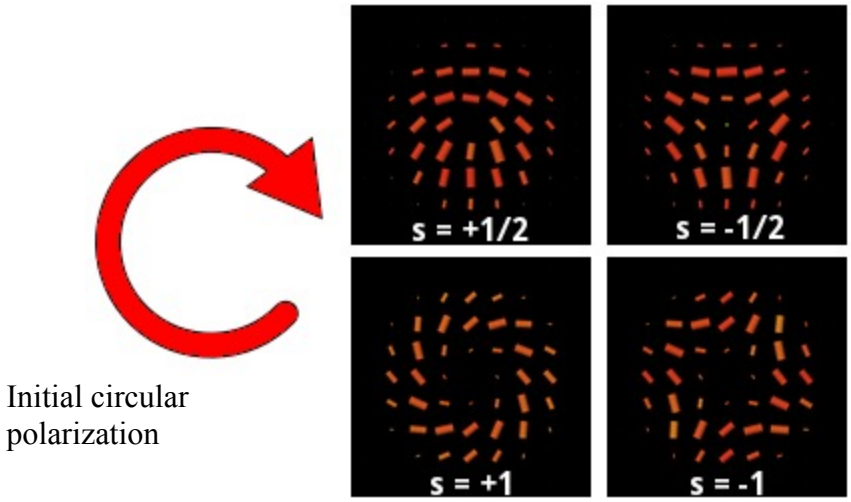

Figure 3. Light defect obtained by shining initially circularly polarized Gaussian light beam along liquid crystal disclination lines with different winding numbers. At a propagation length equal to $z=\lambda/4\Delta n$ (corresponding to phase retardation $\delta=\pi/2$), a defect in the light field with the same winding number as that of the disclination line is obtained. This notably includes half-integer defects. The electric field, as a proper vector, cannot form non-integer defects, but this apparent paradox is resolved by a half-integer phase vortex.

GENERAL LAGUERRE-GAUSSIAN BEAMS

We further explore the relation between defects in liquid crystals and in light by using incident light fields with polarization defects, i.e. Laguerre-Gaussian beams. Again, we observe that the polarization profile effectively changes between two distinct profiles: (i) the profile of the incident beam and (ii) the profile with a winding number equal to (2s-l), where l is the winding number of the incident beam and s the winding number of the disclination line. This relation can be obtained also by using the Jones calculus. In the special case of a Gaussian beam, with l=0, this simplifies to the double-winding-number relation mentioned previously. Combining different nontrivial defects also gives rise to interesting light intensity patterns. Some of these patterns, found when shining an l=+1 beam along a s=-1/2 disclination, are shown in Figure 4. Notably, we see areas of cylindrically-symmetrical intensity profiles, similar to that of the incident beam. However, there are also areas where the intensity profile has an interesting three-fold symmetry, the same symmetry as the disclination line. We thus observe an interesting interplay between the symmetries of the incident beam and the disclination line, not only with the beam polarization profile but also with its intensity.

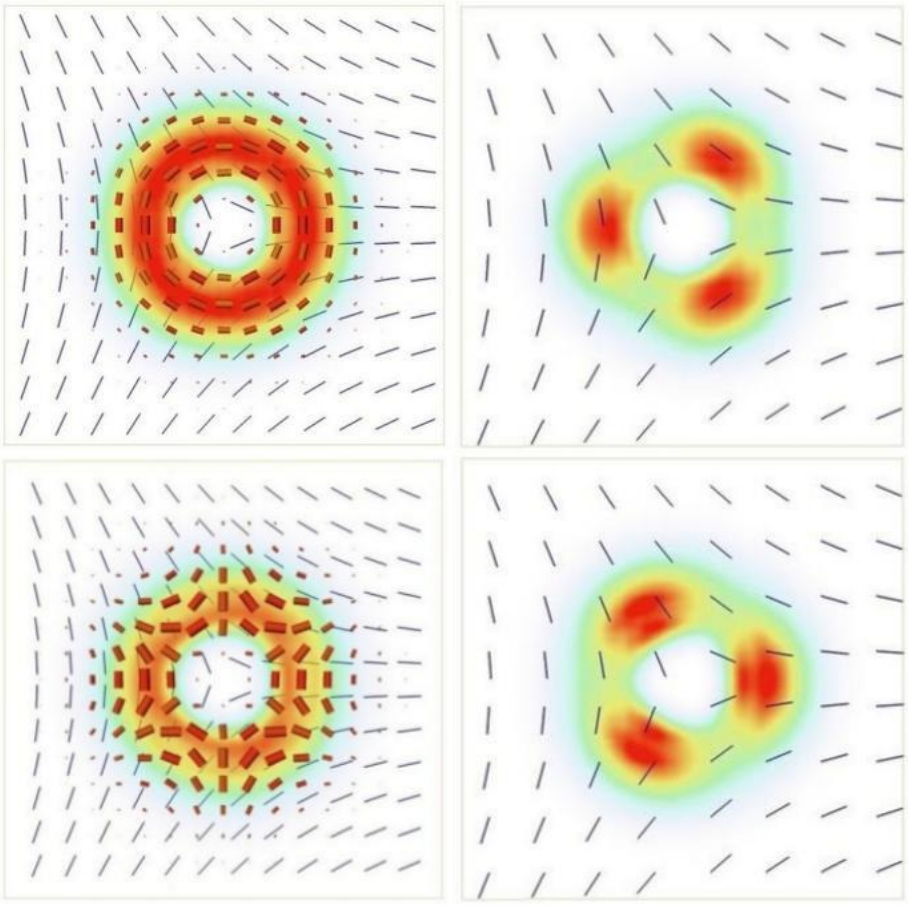

Figure 4. Intensity and polarization of l=1 Laguerre-Gaussian beam propagated along s=-1/2 disclination line. Modulation of both the beam's intensity and polarization profile can be observed. The beam periodically changes between s=+1 state (top left) and s=-2 state (bottom left). Between these states, interchanging patterns with a three-fold symmetry can be observed (right). These results confirm the general case of arbitrary winding numbers, where the light beam alternates between its original state *l* and the transformed state *2s-l.*

MISALIGNED BEAM AND DISCLINATION LINE

In all above cases, the light beams are travelling along the disclination line, and the beam axis is the same as the disclination line core. By changing the beam alignment, i.e. by shining the beam at the disclination at an oblique angle, it is possible to produce novel, less regular intensity and polarization profiles. Instead of traveling along the disclination line through the entire simulation box, the beam covers only a short distance near the defect core, substantially changing its impact on the beam shape. Intensity and polarization profiles of a Gaussian beam crossing a s=-1/2 disclination line at an angle of 30 degrees are shown in Figure 5.

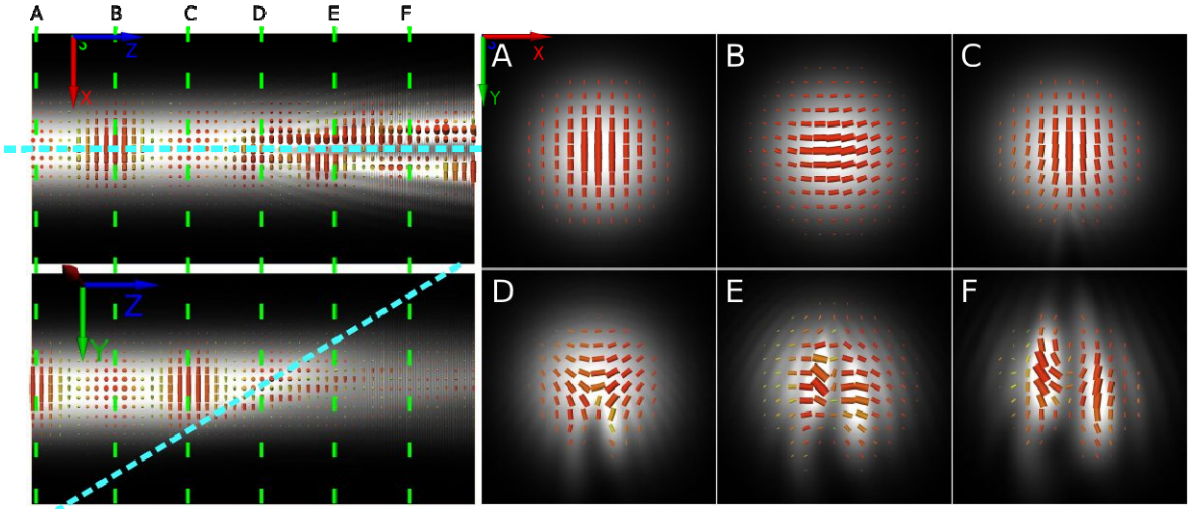

Figure 5. Propagation of a Gaussian light beam when hitting a disclination line at an oblique angle. Views from two sides (left) show light intensity and polarization, along with the disclination line axis (blue dashed lines). Cross sections at different propagation lengths marked with green vertical dashed lines (A-F) show the progression from a uniform polarization profile, through a defect state into disordered profiles with noticeable intensity modulations.

Before hitting the disclination line, the beam travels through a near-uniform birefringent medium, causing its polarization to periodically change from linear to circular and back, while the intensity profile remains unchanged. Near the defect core, however, substantial modulation is observed, causing the beam to change its intensity profile as well. The beam refracts away from the defect core, effectively splitting into two main intensity regions. The polarization profile also changes when traversing the disclination, from a linear profile through a clear s=-1 defect profile, similar to the one that appears when the beam is parallel to the disclination, to a more complicated profile without a clearly discernible structure.

BEAM MODULATION WITH ESCAPED LINES

Escaped disclination lines are interesting for optical applications because of the spatial variation of the observed index of refraction. In a capillary with a circular profile and homeotropic anchoring on the wall, the director forms a radial pattern with the additional escape in the third dimension at the axis. A Laguerre-Gaussian light beam with radial polarization (l=1) will experience the extraordinary refractive index near the capillary wall, and smoothly transition towards the ordinary index at the axis. Note that this only holds true for a beam with a radial polarization profile; the orthogonal mode where light is polarized azimuthally observes the ordinary index everywhere and is unaffected by the director modulation. Escaped disclination lines thus act as polarization selective elements for light.

Nematic liquid crystals typically have extraordinary index of refraction greater than the ordinary one, meaning that the index will be greater near the edges than in the center. As light refracts towards the area with the longer optical path, such a structure will diverge the light beam, as shown in Figure 6.

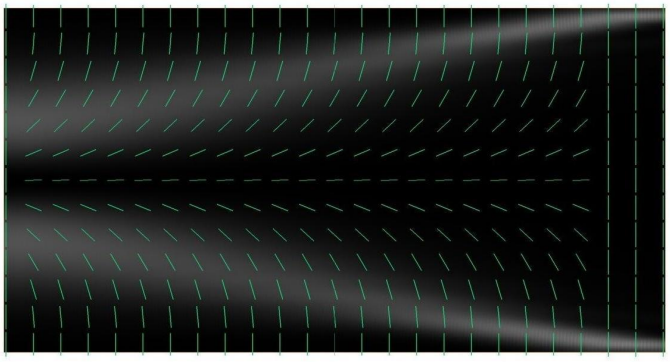

Figure 6. Diverging of a radially polarized light beam along a nematic escaped disclination line. Shades of gray show the light intensity; white marks the areas where the intensity is high, while green lines show the escaped director profile. An orthogonally polarized light beam would pass unaffected, as through an optically uniform material.

CONCLUSIONS

Propagation of Gaussian and Laguerre-Gaussian beams along nematic disclination lines is explored. Numerical modelling based on custom developed Finite Difference Time Domain approach is used to explore the propagation of light beams along spatially varying birefringent profiles, finding nematic defects as capable optical and photonic elements for generation of vector (vortex) light beams. For initially linearly polarized light beams, the nematic disclinations with winding number (charge) *s* generate polarization profiles with defects of winding number *2s*, whereas for initially circularly polarized beams the polarization profiles with defects of winding number *s* emerge. Notably this includes also half-integer defects in the light polarization which is achieved by the formation of the phase vortices in the centre of the beam. The relation between (topological) invariants of the the light and nematic fields is also generalized for Laguerre-Gaussian beams, opening a way to tailoring the intensity and polarization profiles of light beams of various symmetries and profiles. Off-axis propagation of light beam relative to the nematic defect line is shown and propagation along escaped nematic line is considered. Finally, this work is a contribution towards designing soft matter photonics, aiming to use diverse soft matter components and elements –in this paper the nematic defect lines- to control and tune the flow-of-light at the microscopic level.

ACKNOWLEDGMENTS

This research was supported by the Slovenian office of science (ARRS) through grants P1-0099, Z1-5441 and J1-6723.

REFERENCES

[1] Hall, D. G., "Vector-beam solutions of Maxwell's wave equation", Opt. Lett. **21**, 9 (1996)
[2] Zhan, Q., "Cylindrical vector beams: from mathematical concepts to applications", Adv. Opt. Photon. **1**, 1 (2009).
[3] Tovar, A. A., "Production and propagation of cylindrically polarized Laguerre–Gaussian laser beams", J. Opt. Soc. Am. A **15**, 2705 (1998).
[4] Dorn, R., Quabis, S. and Leuchs, G., "Sharper Focus for a Radially Polarized Light Beam", Phys. Rev. Lett. **91**, 233901 (2003).
[5] Zhan, Q., "Trapping metallic Rayleigh particles with radial polarization", Opt. Express **12**, 3377 (2004).
[6] Kawauchi, H., Yonezawa, K., Kozawa, Y. and Sato, S., "Calculation of optical trapping forces on a dielectric sphere in the ray optics regime produced by a radially polarized laser beam", Opt. Lett. **32**, 1839 (2007).

[7] Youngworth, K. and Brown, T., "Focusing of high numerical aperture cylindrical-vector beams", Opt. Express **7**, 77 (2000).
[8] Niziev, V. G. and Nesterov, A. V., "Influence of beam polarization on laser cutting efficiency", J. Phys. D **32**, 1455 (1999).
[9] Kozawa, Y. and Sato, S., "Generation of a radially polarized laser beam by use of a conical Brewster prism", Opt. Lett. **30**, 3063 (2005).
[10] Volpe, G. and Petrov, D., "Generation of cylindrical vector beams with few-mode fibers excited by Laguerre–Gaussian beams", Opt. Commun. **237**, 89–95 (2004).
[11] Shih-Wei Ko, S.-W., Ting, C.-L., A., Fuh, A. Y.-G. and Lin, T.-H., "Polarization converters based on axially symmetric twisted nematic liquid crystal", Opt. Express **18**, 3601 (2010).
[12] Čopar, S., Clark, N. A., Ravnik, M. and Žumer, S., "Elementary building blocks of nematic disclination networks in densely packed 3D colloidal lattices", Soft Matter **9**, 8203 (2013).
[13] Martinez, A., Ravnik, M., Lucero, B., Visvanathan, R., Žumer, S. and Smalyukh, I. I., "Mutually tangled colloidal knots and induced defect loops in nematic fields", Nature Mater. **13**, 258-263 (2014).
[14] Ackerman, P. J., Qi, Z. and Smalyukh, I. I., "Optical generation of crystalline, quasicrystalline, and arbitrary arrays of torons in confined cholesteric liquid crystals for patterning of optical vortices in laser beams", Phys. Rev. E **86**, 021703 (2012).
[15] Ackerman, P. J., van de Lagemaat, J. and Smalyukh, I. I., "Self-assembly and electrostriction of arrays and chains of hopfion particles in chiral liquid crystals", Nature Commun. 6, 6012 (2015).
[16] de Gennes, P. G. and Prost, J.," The Physics of Liquid Crystals, 2nd ed." (Oxford University Press, Oxford, 1995).
[17] Kleman, D. and Lavrentovich, O. D., "Soft Matter Physics: An Introduction" (Springer, New York, 2003).
[18] Čančula, M., Ravnik, M. and Žumer, S., "Generation of vector beams with liquid crystal disclination lines", Phys. Rev. E **90**, 022503 (2014).
[19] Brasselet, E., Murazawa, N., Misawa, H. and Juodkazis, S., "Optical Vortices from Liquid Crystal Droplets", Phys. Rev. Lett. **103**, 103903 (2009).
[20] Loussert, C., Delabre, U. and Brasselet, E., "Manipulating the Orbital Angular Momentum of Light at the Micron Scale with Nematic Disclinations in a Liquid Crystal Film", Phys. Rev. Lett. **111**, 037802 (2013)
[21] Marrucci, L., Manzo, C. and Paparo, D., "Optical Spin-to-Orbital Angular Momentum Conversion in Inhomogeneous Anisotropic Media", Phys. Rev. Lett. **96**, 163905 (2006).
[22] Cardano, F., Karimi, E., Marrucci, L., de Lisio, C. and Santamato, E., "Generation and dynamics of optical beams with polarization singularities", Opt. Express **21**, 8815 (2013)..
[23] Humblet, J., "Sur le moment d'impulsion d'une onde électromagnétique", Physica **10**, 585 (1943).
[24] Nagali, E., Sciarrino, F., Martini, F. D., Piccirillo, B., Karimi, E., Marrucci, L. and Santamato, E., "Polarization control of single photon quantum orbital angular momentum states", Opt. Express **17**, 18745 (2009).
[25] Cardano, F., Karimi, E., Slussarenko, S., Marrucci, L., de Lisio, C. and Santamato, E., "Polarization pattern of vector vortex beams generated by *q*-plates with different topological charges", Appl. Opt. **51**, C1 (2012).
[26] Brasselet, E., "Singular optical reordering of liquid crystals using Gaussian beams", J. Opt. **12**, 124005 (2010).
[27] Porenta, T., Ravnik, M. and Žumer, S., "Complex field-stabilised nematic defect structures in Laguerre–Gaussian optical tweezers", Soft Matter **8**, 1865 (2012).
[28] Assanto, G., "Nematicons: Spatial Optical Solitons in Nematic Liquid Crystals" (John Wiley & Sons, 2012)
[29] Taflove, A. and Hagness, S. C., "Computational Electrodynamics: The Finite-Difference Time-Domain Method" (Artech House, Norwood, MA, 2005).
[30] Yee, K., "Numerical solution of initial boundary value problems involving maxwell's equations in isotropic media ", IEEE Trans. Antenna Propag. **14**, 302 (1966).
[31] Oskooi, A. F., Roundy, D., Ibanescu, M., Bermel, P., Joannopoulos, J. and Johnson, S. G., "Meep: A flexible free-software package for electromagnetic simulations by the FDTD method", Comput. Phys. Commun. **181**, 687 (2010).
[32] Werner, G. R. and Cary, J. R., "A stable FDTD algorithm for non-diagonal, anisotropic dielectrics", J. Comput. Phys. **226**, 1085 (2007).
[33] Berenger, J.-P., "A perfectly matched layer for the absorption of electromagnetic waves", J. Comput. Phys. **114**, 185 (1994).
[34] Ravnik, M. and Žumer, S., "Landau-de Gennes modelling of nematic liquid crystal colloids", Liq. Cryst. **36**, 10 (2009).
[35] Hecht, E., "Optics" (Addison-Wesley Longman, 2002).